Inorganic Chemistry

pubs.acs.org/IC Article

Ru(II)-Based Acetylacetonate Complexes Induce Apoptosis Selectively in Cancer Cells

Sayak Gupta, Jessica M. Vandevord, Lauren M. Loftus, Nicholas Toupin, Malik H. Al-Afyouni, Thomas N. Rohrabaugh, Jr., Claudia Turro,* and Jeremy J. Kodanko*



Cite This: Inorg. Chem. 2021, 60, 18964-18974



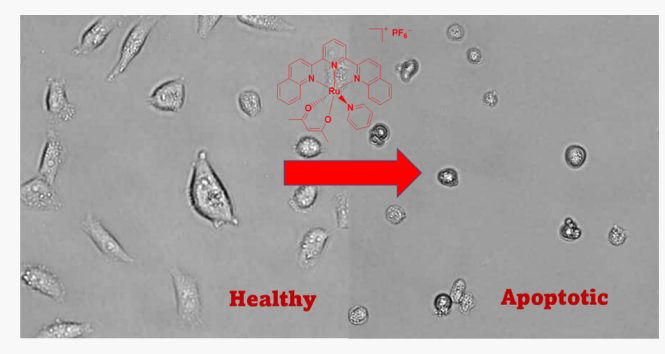
ACCESS

Metrics & More



Supporting Information

ABSTRACT: The synthesis, chemical and biological characterization of seven Ru(II) polypyridyl complexes containing acetylacetonate (acac) ligands are reported. Electronic absorption spectra were determined and electrochemical potentials consistent with Ru(III/II) couples ranging from +0.60 to +0.73 V vs Ag/AgCl were measured. A series of complexes were screened against MDA-MB-231, DU-145, and MCF-10A cell lines to evaluate their cytotoxicities in cancer and normal cell lines. Although most complexes were either nontoxic or equipotent in cancer cells and normal cell lines, compound 1, [Ru(dpqy)(acac)(py)](PF₆), where dqpy is 2,6-di(quinolin-2-yl)pyridine, showed up to 2.5:1.0 selectivity for cancer as compared to normal cells, along with



nanomolar EC₅₀ values in MDA-MB-231 cells. Lipophilicity, determined as the octanol/water partition coefficient, $\log P_{\text{o/w}}$, ranged from -0.33~(0.06) to 1.15~(0.10) for the complexes. Although cytotoxicity was not correlated with electrochemical potentials, a moderate linear correlation between lipophilicity and toxicities was observed. Cell death mechanism studies indicated that several of the Ru–acac compounds, including 1, induce apoptosis in MDA-MB-231 cells.

■ INTRODUCTION

Cancer is the second leading cause of human death around the world. According to the World Health Organization (WHO), cancer was responsible for roughly 9.6 million deaths in 2018 alone. One of the most common methods to treat cancer is chemotherapy, which involves the administration of drugs to induce cancer cell death. However, a significant drawback of all chemotherapeutics is their lack of selectivity, resulting in toxicity toward both healthy and malignant tissues. Low selectivity leads to many undesirable side effects, including neurotoxicity, nephrotoxicity, nausea, vomiting, and hemolytic anemia.

Platinum-based drugs are a prominent group of chemotherapeutics used to treat roughly 50% of human cancers. Cisplatin has been approved to treat cancer since the 1970s, with carboplatin and oxaliplatin approved later. While very successful in cancer treatment, the severe side effects of platinum-based drugs have inspired the quest to find new metal-based compounds as alternatives for cancer treatment. Transition-metal complexes derived from osmium, ruthenium, and rhodium have been investigated as metal-based anticancer agents and alternatives to platinum-based drugs. From these investigations, Ru-based metal complexes have emerged as promising leads. Ruthenium-based therapeutics have shown reduced *in vivo* toxicity compared to those derived from Pt(II), which is believed to stem from the ability of some

ruthenium complexes to mimic iron in binding with serum albumin and transferrin proteins in the body. 19,20 Both Ru(II) and Ru(III) complexes have been investigated as anticancer agents. For the latter, the reducing environment of cancer cells is proposed to lead to the reduction of Ru(III) to Ru(II), leading to selectivity of this class of compounds toward cancer cells that contain a more reducing environment than healthy cells. 19,20 One manner in which Ru(II) complexes lead to cell death is through interactions with DNA. 21,22

Several ruthenium complexes have advanced to clinical trials, including NAMI-A, KP1019, NKP-1339, and TLD1433 (Figure 1). PRP1019 causes cell death by attacking the mitochondria, whereas NAMI-A disrupts cell invasion and metastasis. Photodynamic therapy (PDT) involves the activation of nontoxic photosensitizers by the light of suitable wavelength and produces singlet oxygen ($^{1}O_{2}$) or other reactive oxygen species (ROS), resulting in cellular damage in the irradiated tissue. TLD1433 is one example of a Ru(II) complex currently in a Phase II clinical trial as a PDT

Received: September 8, 2021 Published: November 30, 2021





Figure 1. Examples of Ru complexes previously investigated as anticancer agents, including NAMI-A, NKP-1339, and TLD1433 that entered clinical trials.

agent.^{25,26} Other ruthenium complexes that have undergone extensive preclinical studies include RAPTA-C and RAPTA-T and show excellent *in vivo* antitumor activities (Figure 1).²⁷ The ability of ruthenium complexes to achieve cell death through many different pathways makes them versatile candidates as cancer therapeutics.

Although many Ru(II) complexes have been investigated as anticancer agents in vitro, those that elicit cancer cell death in the nanomolar range in vitro are rare. Most Ru(II) complexes induce cancer cell death in the single-digit micromolar range, similar to cisplatin. Ru(II) polypyridyl complexes with different types of dioxo ligands have shown promise as potential anticancer agents. Among those Ru(II) polypyridyl complexes, analogues with acetylacetonate-based ligands have been particularly active. Ru(II) complexes with the general formula $[Ru(bpy)_2(L)]^+$, where bpy = 2,2'-bipyridine and L is a diverse array of κ^2 -O-O' chelating β -diketone ligands including acetylacetonate (acac), showed nanomolar potency against DU-145 cells (human prostate cancer) and MIA PaCa-2 cells (human pancreatic cancer).³⁹ In vivo toxicity of these complexes was evaluated in a zebrafish model, where data indicated that most complexes were nontoxic in vivo. Curcumin (a type of κ^2 -O-O' chelating β -diketone ligand)based polypyridyl Ru(II) complexes with formulae [Ru-(bpy)₂(curcumin)]⁺ and [Ru(bpy)(dppn)(curcumin)]⁺, where dppn = benzo[i]dipyrido[3,2-a:2',3'-c]phenazine, showed single-digit micromolar potency against A549, MCF-7, and SGC7901 cell lines.³⁷ Recently, several bpy-based Ru(II) complexes with a coordinated ferrocenyl β -diketonate (Fc-acac) ligand have been reported. These complexes showed

nanomolar potency against MIA PaCa-2 (human pancreatic cancer cells) and HCT116 p53 $^{+/+}$ (p53 wild-type human colon cancer cells). Studies on DNA damage with these complexes revealed that they are able to cause DNA cleavage.³⁶

In this paper, we report the synthesis and biological characterization of Ru(II) polypyridyl complexes containing acac-based ligands. The spectral and electrochemical properties of these Ru—acac complexes were characterized. This series of compounds was evaluated against two cancer cell lines and one non-cancer cell line to characterize their selectivities toward cancer cells. We observed that two out of our seven complexes displayed potent toxicity, one of which showed cell death in the nanomolar range and up to 2.5-fold selectivity toward triple-negative breast cancer cells as compared to a normal breast epithelial cell line. Studies on cell death mechanisms on two lead agents revealed that they induced apoptosis in triplenegative breast cancer cells. This study exposes rich structure—activity relationships in Ru—acac complexes that warrant their further investigation as anticancer agents.

EXPERIMENTAL SECTION

Materials. All materials were used as received without further purification unless noted otherwise. Diethyl ether was purchased from Fisher Scientific, while anhydrous ethanol was obtained from Decon Laboratories. All deuterated solvents and N-bromosuccinimide were purchased from Sigma-Aldrich; pyridine was obtained from Mallinckrodt Chemicals; N-chlorosuccinimide was purchased from Alfa Aesar; and ammonium hexafluorophosphate was obtained from Acros Organics. The starting materials [Ru(dqpy)(acac)Cl], [Ru(tpy)(acac)Cl] (tpy = 2,2':6',2''-terpyridine), $[Ru(bpy)_2Cl_2]$, and

[Ru(tpy)(thd)Cl] (thd = 2,2,6,6-tetramethylheptane-3,5-dionate), as well as 2, were prepared by following literature methods. $^{40-43}$

Instrumentation. ¹H NMR spectra were collected using a Bruker DPX 400 MHz spectrometer in the indicated deuterated solvent, and all chemical shifts were referenced to the residual protonated solvent peak ((CD₃)₂CO = 2.05 ppm, (CD₃)₂SO = 2.50 ppm). ⁴⁴ Electrospray ionization (ESI) mass spectrometry was performed using a Bruker microTOF instrument in a positive mode with methanol as the eluent. Electrochemical experiments were carried out on a BASi model CV-50W voltammetric analyzer (Bioanalytical Systems, Inc.; West Lafayette, IN). Cyclic voltammetry (CV) experiments were carried out with solutions containing 0.5 mM of each complex with a glassy carbon disk working electrode (3 mm diameter), platinum wire auxiliary electrode, and Ag/AgCl (3 M NaCl) reference electrode (calibrated with ferrocene; Fc^{0/+} = 0.438 vs Ag/AgCl), and the solutions were purged with N₂ prior to each trial.

Synthesis of [Ru(dpqy)(acac)(py)](PF₆) (1). Ru(dqpy)(acac)Cl (44.9 mg, 0.0789 mmol) was dissolved in 20 mL of a 1:1 EtOH/H₂O mixture. Pyridine (1 mL, excess) was added to the mixture and the solution was allowed to reflux under a nitrogen atmosphere in the dark for 24 h. The purple reaction mixture was allowed to cool to room temperature, concentrated *in vacuo*, and added to an aqueous solution of NH₄PF₆ (0.1333 g in 100 mL). The resulting solid was collected by vacuum filtration, washed with H₂O and with diethyl ether, and dried to yield 1 as a dark purple solid (27.5 mg, 57%). ¹H NMR (400 MHz, (CD₃)₂CO): δ 9.23 (d, 2H, 9.73), 8.91 (d, 2H, 8.17), 8.74 (d, 2H, 8.88), 8.63 (d, 2H, 8.52), 8.48 (d, 2H, 5.68), 8.19 (t, 1H, 7.46), 8.12 (d, 2H, 7.81), 7.98 (t, 2H, 7.85), 7.81 (t, 2H, 7.85), 7.47 (t, 1H, 7.32), 7.00 (t, 2H, 6.80), 5.46 (s, 1H), 2.74 (s, 3H), and 1.27 (s, 3H) ppm. ESI-MS(+): [M – PF₆]⁺ experimental m/z = 613.12, calculated m/z = 613.12.

Synthesis of [Ru(tpy)(acac)(py)](PF₆) (3). [Ru(tpy)(acac)Cl] (125 mg, 0.267 mmol) was dissolved in 50 mL of a 1:1 EtOH/H₂O mixture. Pyridine (2 mL, excess) was added to the mixture, and the solution was allowed to reflux under a nitrogen atmosphere in the dark for 15 h. The purple reaction mixture was allowed to cool to room temperature, concentrated *in vacuo*, and added to an aqueous solution of NH₄PF₆ (0.1 g in 100 mL). The resulting solid was collected by vacuum filtration, washed with H₂O, and dried with diethyl ether to yield 3 as a dark purple solid (157 mg, 89%). ¹H NMR (400 MHz, (CD₃)₂CO): δ 8.68 (ddd, 2H, J = 5.4, 1.3, 0.6 Hz), 8.60 (m, 4H), 8.12 (m, 4H), 7.96 (t, 1H, J = 8.0 Hz), 7.72 (ddd, 2H, J = 7.5, 5.6, 1.3 Hz), 7.61 (tt, 1H, J = 7.6, 1.4 Hz), 7.11 (ddd, 2H, J = 7.5, 5.4, 1.3 Hz), 5.47 (s, 1H), 2.47 (s, 3H), and 1.39 (s, 3H) ppm. ESI-MS(+): [M – PF₆]⁺ experimental m/z = 513.08.

Synthesis of [Ru(tpy)(thd)(py)](PF₆) (4). This complex was prepared in the same fashion as 3 using [Ru(tpy)(thd)Cl] (44 mg, 0.080 mmol) in an EtOH/H₂O mixture (1:1, 24 mL) with 1 mL of pyridine (excess) and an aqueous solution of NH₄PF₆ (0.1 g in 100 mL) to yield 4 as a dark purple solid (51 mg, 85%). ¹H NMR (400 MHz, (CD₃)₂CO): δ 8.62 (d, 2H, J = 8.1 Hz), 8.61 (d, 2H, J = 8.1 Hz), 8.58 (ddd, 2H, J = 5.5, 1.5, 0.8 Hz), 8.21 (ddd, 2H, J = 5.2, 1.4, 1.4 Hz), 8.11 (ddd, 2H, J = 7.8, 7.8, 1.5 Hz), 7.96 (t, 1H, J = 8.0 Hz), 7.72 (ddd, 2H, J = 7.6, 5.5, 1.4 Hz), 7.63 (tt, 1H, J = 7.6, 1.5 Hz), 7.16 (ddd, 2H, J = 7.6, 5.3, 1.3 Hz), 5.79 (s, 1H), 1.54 (s, 9H), and 0.54 (s, 9H) ppm. ESI-MS(+): [M - PF₆]⁺ experimental m/z = 597.17, calculated m/z = 597.18.

Synthesis of [Ru(tpy)(Cl-acac)(py)](PF₆) (5). [Ru(tpy)(acac)(py)]-(PF₆) (75.2 mg, 0.114 mmol) and N-chlorosuccinimide (23.0 mg, 0.172 mmol) were dissolved in 10 mL of dichloromethane, which was purified using a MBraun solvent purification system. The solution was allowed to stir in the dark for 2 h, then NH₄PF₆ (~0.09 g) was added, and the solvent was then removed *in vacuo*. The solid was purified via column chromatography (silica, dichloromethane/acetonitrile, 9:1) (58.2 mg, 74%). ¹H NMR (400 MHz, (CD₃)₂CO): δ 8.74 (ddd, 2H, J = 5.5, 1.5, 0.8 Hz), 8.63 (m, 4H), 8.15 (m, 4H), 8.01 (t, 1H, J = 8.1 Hz), 7.74 (ddd, 2H, J = 7.6, 5.5, 1.3 Hz), 7.63 (tt, 1H, J = 7.7, 1.5 Hz), 7.14 (ddd, 2H, J = 7.6, 5.3, 1.3 Hz), 2.74 (s, 3H), and 1.67 (s,

3H) ppm. ESI-MS(+): $[M - PF_6]^+$ experimental m/z = 547.05, calculated m/z = 547.05.

Synthesis of [*Ru(tpy)(Br-acac)(py)](PF₆)* (*6*). This complex was prepared in the same fashion as 5 using [Ru(tpy)(acac)(py)](PF₆) (50 mg, 0.076 mmol) and *N*-bromosuccinimide (14 mg, 0.0786 mmol) in 10 mL of purified dichloromethane to produce dark purple solid (45.0 mg, 78%). ¹H NMR (400 MHz, (CD₃)₂CO): δ 8.75 (ddd, 2H, J = 5.5, 1.5, 0.7 Hz), 8.64 (m, 4H), 8.15 (m, 4H), 8.01 (t, 1H, J = 8.1 Hz), 7.75 (ddd, 2H, J = 5.5, 1.5, 0.8 Hz), 7.63 (tt, 1H, J = 7.6, 1.5 Hz), 7.14 (ddd, 2H, J = 7.5, 5.4, 1.3 Hz), 2.84 (s, 3H), and 1.76 (s, 3H) ppm. ESI-MS(+): [M - PF₆]⁺ experimental m/z = 590.99, calculated m/z = 590.99.

Synthesis of $[Ru(dqpy-COOH)(acac)(py)](PF_6)$ (7). $[Ru(dqpy-COOH)(acac)(py)](PF_6)$ COOH)(acac)Cl] (49.8 mg, 0.0657 mmol) was dissolved in 20 mL of a 1:1 EtOH/H2O mixture. Pyridine (3 mL, excess) was added to the mixture and the solution was allowed to reflux under a nitrogen atmosphere in the dark for 24 h. The purple reaction mixture was allowed to cool to room temperature, and $\ensuremath{\mathsf{HNO}}_3$ was added until the solution was at a pH < 1. The solution was then concentrated in vacuo and added to an aqueous solution of NH₄PF₆ (0.1333 g in 100 mL). The resulting solid was collected by vacuum filtration, washed with H₂O and diethyl ether, and dried to yield 7 as a dark purple solid (26.3 mg, 50%). ¹H NMR (400 MHz, (CD₃)₂SO): δ 9.17 (s, 2H), 8.98 (d, 2H, J = 8.97 Hz), 8.89 (d, 2H, J = 8.93), 8.62 (d, 2H J =8.93), 8.21 (d, 2H, J = 5.68), 8.11 (d, 2H, J = 8.12), 7.94 (t, 2H, J = 8.12) 7.85), 7.77 (t, 2H, J = 7.31), 7.43 (t, 1H, J = 7.58), 6.99 (t, 2H, J = 7.85) 6.76), 5.40 (s, 1H), 2.67 (s, 3H), and 1.23 (s, 3H) ppm. ESI-MS(+): $[M - PF_6]^+$ experimental m/z = 658.11, calculated m/z = 658.12.

Preparation of the Growth Medium. The growth medium of DU-145 and MDA-MB-231 cell lines were prepared by adding 50 mL of FBS and 5 mL of penicillin/streptomycin (1000 units/mL) in 500 mL of Eagle's minimum essential medium (EMEM) and Dulbecco's modified Eagle's medium (DMEM), respectively. The MCF-10A cell line growth medium was prepared by adding 25 mL of 5% horse serum, 100 μ L of 20 ng/mL EGF, 250 μ L of 0.5 mg/mL hydrocortisone, 50 μ L of 100 ng/mL cholera toxin, 500 μ L of 10 μ g/mL insulin, and 5 mL of penicillin/streptomycin to 500 mL of Dulbecco's modified Eagle's medium (DMEM).

Determination of EC₅₀ Values. The cell viability of all of the synthesized complexes were determined by plating the cells of a respective cell line (DU-145, MDA-MB-231, or MCF-10A) in a 96well plate at a density of 7000 cells per well in the growth medium for that particular cell line. The plates were incubated overnight in a 37 °C humidified incubator ventilated with 5% CO₂. The growth media was aspirated off, and then quadruplicate wells were treated with growth media containing different concentrations (25 μ M to 100 nM) of the synthesized complexes in 1% DMSO. Plates containing wells with no cells were designated as blank wells, whereas wells with cells that were not treated with the compound but only with growth media containing 1% DMSO (vehicle) were designated as control wells. The plates were then again incubated in a 37 °C humidified incubator ventilated with 5% CO₂. After 1 h of incubation, the growth media in each well were aspirated off and replaced with new growth media. The plates were finally incubated in a 37 °C humidified incubator ventilated with 5% CO₂ for 72 h. After incubation, 10 μ L of the MTT (3-(4,5-dimethylthiazol-2-yl)-2,5-diphenyltetrazolium bromide) reagent (5 mg/mL in PBS) was added to each well of the 96-well plate and incubated in a 37 °C humidified incubator ventilated with 5% CO₂ for 2 h. After 2 h, the media were aspirated off and 100 μ L of DMSO was added. The plates were then shaken for 20 min to ensure complete dissolution of purple formazan crystals. The absorbance of each well was then measured at 570 nm. The mean absorbance values of the blank wells were calculated and subtracted from the absorbance values for each well treated with a certain concentration of a compound. The absorbance of the control wells was also taken and subtracted with the average of the blank wells. The mean of these corrected control absorbances was then calculated. Viability of the cells was finally determined by dividing the corrected absorbance of the compound wells by the mean corrected absorbance of the blank wells and expressing the mean of the ratio as a percentage value.

Viabilities as percentages were plotted against the log of concentration (M) of the compounds, and the antilog of the concentration value at 50% viability gave us the EC₅₀ of the particular compound in a specific cell line

Stability Studies. To study the stability of the complexes over time, solutions of 1–7 (10 μ M) were prepared in phenol red-free Dulbecco's modified Eagle's medium (DMEM) at room temperature. Immediately after the preparation of the solutions, electronic absorption spectra were collected. The samples were kept in an incubator at 37 °C for 24 h and then allowed to attain room temperature. Electronic absorption spectra of all of the solutions were again collected. The samples were then kept in an incubator at 37 °C for another 24 h and allowed to attain room temperature. Lastly, a final round of electronic absorption spectra was acquired.

Determination of the Mechanism of Cell Death by Cotreatment with Complexes and Inhibitors. The mechanism of cell death was studied for complexes 1 and 4 in MDA-MB-231 cell lines. MDA-MB-231 cells were taken in 96-well plates and pretreated with 50 μ L of growth media containing 10 μ M necrostatin (NEC), 20 μM Z-VAD-FMK (Z-VAD), and 5 mM N-acetylcysteine (NAC) in sextuplicate after aspirating off the growth media already present. The plates also contained blank wells with no cells and control wells. One column of wells in the plate along with the blank and control wells was treated with 50 µL of growth media with 1% DMSO (vehicle). The plates were incubated in a 37 °C humidified incubator ventilated with 5% CO₂ for 1 h. The plates were then taken out of the incubator and 50 μ L of either complex 1 (600 nM) or 4 (4 μ M) was added to the column of wells that were pretreated with the vehicle along with half the wells pretreated with 10 μM necrostatin, 20 μM Z-VAD-FMK, or 5 mM N-acetylcysteine. Then, 50 μ L of the vehicle was added to the rest of the wells that were pretreated with 10 μM necrostatin, 20 µM Z-VAD-FMK, or 5 mM N-acetylcysteine along with the blank and control wells. The plates were then incubated in a 37 °C humidified incubator ventilated with 5% CO₂ for 72 h, after which the viability of the cells was studied using MTT assay.

Determination of log *P*. Solutions of complexes 1-7 (3 mL, 40 μ M) were prepared in octanol. To the same container, 3 mL of deionized water was added. The containers were shaken vigorously for 5 min and allowed to settle overnight for complete separation of water and octanol layers. Three absorbance readings of both the octanol and water layers were then collected for each complex. The log *P* value of each complex was finally determined by taking the log of the ratio of the mean absorbance in the octanol layer to the mean absorbance in the water layer.

Fluorescence-Assisted Cell Sorting (FACS) Studies. MDA-MB-231 cells were seeded at 250 000 cells/plate in six 60 mm² cell culture dishes containing 3 mL of DMEM treated with 10% FBS and 1000 units/mL penicillin/streptomycin. After seeding, the cells were incubated at 37 °C and 5% CO₂ overnight (18 h). After incubation, plates were treated with either compound 1 (300 nM or 1 μ M) or 4 (3 or 6 μ M) in media (1% DMSO) and set to incubate at 37 °C and 5% CO₂ for 72 h. The remaining two plates were treated with DMEM containing 1% DMSO and placed in the incubator. After incubation, plates were removed from the incubator. In a separate plate, after 2 h, cells treated with vehicle alone had media removed and replaced with H₂O₂ (500 mM) in PBS. The cells were incubated at 37 °C and 5% CO₂ for 3 h. The media from each plate was saved in a 15 mL falcon tube. The cells were detached from each plate via trypsinization and added to the previously removed media. The cells were centrifuged (600g, 5 min) to pellet the cells. The supernatant was decanted, and the pellet was washed with PBS (2 mL) followed by another wash with annexin binding buffer (2 mL). After the final wash, the supernatant was decanted, and the pellet was suspended in annexin binding buffer (100 μ L). A solution of annexin V (5 μ L, 1 mg/mL) was added to the cell suspension. The suspension was incubated at rt (15 min). After incubation, annexin binding buffer was added (1 mL) to the tube and the suspension was centrifuged (600g, 5 min). The supernatant was decanted, and cells were suspended in annexin binding buffer (100 µL). A solution of propidium iodide (5 µL, 12 μ M) was added to the cell suspension and incubated at rt (15 min).

The cell suspension was diluted with annexin binding buffer (1 mL). The suspension was passed through a metal mesh filter (30 μ m) from Celltrics (Kobe, Hyogo Prefecture, Japan) into a small sample tube. Flow cytometric analysis was performed on a Sysmex Cyflow Space fluorescence-assisted cell sorter. Data were processed using FCS Express.fcs processing software by De Novo software (Boulder, Co).

RESULTS

Synthesis and Characterization of Ru–acac Complexes. Seven Ru(II) polypyridyl complexes incorporating acac-based ligands were examined in this study. Structures for the seven complexes are shown in Figure 2. Pyridine (py) is a

Figure 2. Molecular structures of the Ru-acac series 1-7.

common monodentate ligand present in 1 and 3–7. Complexes 3–5 and 6 contain 2,2':6',2''-terpyridine (tpy) as a polypyridyl ligand. Complexes 3, 5, and 6 all carry the [Ru(tpy)(py)] fragment with acac, Cl-acac (3-chloroacetylacetonate), and Br-acac (3-bromoacetylacetonate), respectively. In complex 4, [Ru(tpy)(py)(thd)](PF₆) (thd = 2,2,6,6-tetramethylheptane-3,5-dione), the thd ligand replaces acac in 3. Complex 2 is the only compound in the series that does not contain a monodentate pyridine but instead is coordinated by two 2,2'-bipyridine (bpy) polypyridyl ligands along with one acac group. Complex 1 contains the 2,6-di(quinolin-2-yl)pyridine (dqpy) ligand and the dqpy in 7 is adorned with a carboxylic acid group at the 4-position on pyridine (Figure 2).

Complex 2 was prepared by a literature method; ⁴⁵ compounds 1 and 3–7 were synthesized as shown in Scheme 1. Derivatives 1 and 7 were prepared by treating their respective Ru monochloride precursors with excess pyridine in 1:1 EtOH/H₂O at reflux for 24 h, giving 1 and 7 in 57% and 50% yield, respectively (Scheme 1A). Complexes 3 and 4 were prepared in a similar manner by treating [Ru(tpy)(acac)Cl] or [Ru(tpy)(thd)Cl] with excess pyridine in 1:1 EtOH/H₂O at reflux for 24 h, providing 3 and 4 in 89% and 85% yield, respectively (Scheme 1B). ⁴⁰ Compounds 5 and 6 were accessed from 3 in 74 and 78% yield, respectively, through the selective halogenation of the acac ligand using *N*-chlorosuccinimide or *N*-bromosuccinimide in CH₂Cl₂ (Scheme 1C).

Scheme 1. Synthesis of Ru-acac Complexes 1 and 3-7

(A)
$$CI$$
 $R_1 = H \text{ or } CO_2H$

(B) $R_1 = H \text{ or } CO_2H$

(B) $R_2 = CH_3 \text{ or } t\text{-Bu}$

(C) $R_2 = CH_3 \text{ or } t\text{-Bu}$

(C) $R_2 = CH_2CI_2$
 $R_3 = CH_2CI_2$

(C) $R_4 = CH_2CI_2$

(D) $R_5 = CH_2CI_2$

(E) $R_5 = CH_2CI_2$

(F) $R_5 = CH_2CI_2$

The electronic absorption spectra of 2-6 exhibit metal-to-ligand charge transfer (MLCT) absorption with maxima in the 539–555 nm range, corresponding to $Ru(d\pi) \rightarrow tpy(\pi^*)$ transitions in 3-6, $Ru(d\pi) \rightarrow dqpy(\pi^*)$ in 1 and 7, and $Ru(d\pi) \rightarrow bpy(\pi^*)$ in 2. As expected from the previous work on related CH₃CN-coordinated complexes with acac, Cl-acac, and Br-acac ligands, the lowest energy MLCT maxima of 5 and 6 are slightly blue-shifted as compared to that of $3.^{40}$ Importantly, the two lowest energy MLCT transitions of 1 and 7 are observed at ~733 and 809 nm, which lie in the PDT window for excitation that better penetrates tissue. This red shift arises from the more extended π -system of the dqpy ligand as compared to tpy, lowering the energy of the π^* lowest unoccupied molecular orbital (LUMO) of the former.

Prior investigations with Ru(II) polypyridyl complexes revealed a correlation between the redox potentials of the compounds and their behavior in cancer cells. 46 Therefore, the electrochemical half-wave reduction potentials of 1-7, $E_{1/2}$, were measured in CH3CN and are listed in Table 1. Cathodic waves were observed for 1-7 in the range of +0.60 to +0.73 V vs Ag/AgCl and are consistent with a Ru(III/II) couple as is typical of ruthenium polypyridyl complexes.⁴⁷ It should be noted, however, that π -donating acac ligand and its derivatives mix with the Ru t_{2e}-type highest occupied molecular orbital (HOMO), raising its energy. This mixing, along with the overall +1 charge in 1-7, leads to the acac complex being more easily oxidized than the corresponding divalent bpy complexes. For example, [Ru(tpy)(acac)(dmso)]⁺ is oxidized at a potential 0.72 V more negative than [Ru(tpy)-(bpy)(dmso)]²⁺. ⁴⁸ The one-electron reduction of 2 is known to place an electron on one of the bpy ligands, at a potential that is typical for bpy reduction.⁴⁷ Similarly, the tpy ligand is

Table 1. Electronic Absorption Maxima, λ_{abs} , Molar Extinction Coefficients, ε , and Half-Wave Reduction Potentials for 1–7 in CH₂CN

complex	$\lambda_{ m abs}/{ m nm}~(arepsilon/{ m M}^{-1}~{ m cm}^{-1})$	$E_{1/2}/V^a$				
1	570 (4740), 595 (4740), 734 (1100), 809 (1020)	+0.73, -1.16				
2	374 (11 670), 522 (9535), ~570 (sh)	+0.66, -1.48				
3	370 (10 440), ~500 (sh), 551 (4920)	+0.66, -1.43				
4	373 (12 940), ~520 (sh), 551 (6370)	+0.60, -1.48				
5	369 (12 400), ~500 (sh), 537 (6310)	+0.70, -1.42				
6	371 (13 360), ~490 (sh), 539 (6380)	+0.69, -1.42				
7	555 (4740), ~595 (sh), 732 (1150), 809 (980)	+0.73, -1.21				
^a vs Ag/AgCl in CH ₃ CN (0.1 M TBAPF ₆).						

reduced in 3–6 in the -1.42 to -1.48 V range vs Ag/AgCl, whereas this potential shifts to -1.16 and -1.21 V vs Ag/AgCl in 1 and 7, respectively. As expected, the dqpy ligand is more easily reduced than tpy owing to its more expanded π -system, a result consistent with the red shift in the MLCT bands of 1 and 7 as compared to those observed for 3–6.

Biological Evaluation of Ru–acac Complexes. The series of Ru(II) compounds 1–7 were evaluated against two cancer cell lines, DU-145 (human prostate cancer cells) and MDA-MB-231 (human triple-negative breast cancer cells), along with one normal cell line, MCF-10A (nontumorigenic breast epithelial cells). EC₅₀ values were determined for each compound in the three cell lines (Table 2). From the EC₅₀ data, it is clear that compound 1 was the most potent in the series and the only compound to show an EC₅₀ value below 1 μ M in MDA-MB-231 cells (Table 2). Although 1 was less potent in DU-145 cancer cells, it was also less potent in the normal breast epithelial line MCF-10A, resulting in a selectivity

Table 2. EC_{50} Values^a and $\log P_{\text{o/w}}^{\ \ b}$ of 1–7 in Different Cell Lines along with Their Corresponding MDA-MB-231 Selectivity Values, $EC_{50}(\text{MCF-}10A)/EC_{50}(\text{MDA-MB-}231)$, and DU-145 Selectivity Values, $EC_{50}(\text{MCF-}10A)/EC_{50}(\text{DU-}145)$

	$\mathrm{EC}_{50}/\mu\mathrm{M}$					
complex	MDA-MB-231	DU-145	MCF-10A	MDA-MB-231 selectivity	DU-145 selectivity	$\log P_{ m o/w}$
1	0.67 (0.10)	1.2 (0.1)	1.7 (0.3)	2.5	1.41	1.15 (0.10)
2	>25	>25	>25			-0.17 (0.04)
3	17.7 (0.4)	>25	>25	>1.4		-0.33 (0.06)
4	2.5 (0.3)	3.4 (0.4)	3.7 (0.7)	1.50	1.08	0.79 (0.11)
5	8.7 (1.7)	9.9 (0.9)	7.4 (1.6)	0.90	0.74	0.52 (0.08)
6	9.7 (1.1)	10.1 (0.3)	11.1 (0.2)	1.1	1.09	0.78 (0.13)
7	>25	>25	>25			0.99 (0.15)

"Data are average of three independent experiments with quadruplicate wells; errors reported as standard deviations are shown in parentheses; MDA-MB-231, DU-145, or MCF-10A cells were seeded (7000 cells per well) in 96-well plates, plates were incubated overnight, then treated with respective growth media containing complexes 1-7 (0.01–25 μ M), and allowed to incubate at 37 °C for 1 h. After 1 h, growth media was removed and new growth media was added; cells were incubated for 72 h. Viabilities of cells were measured by MTT assay and converted to percentages vs treatment with growth media for fitting EC₅₀ curves. ^bData are an average of three different experiments; see the Experimental Section for more details.

factor of 2.5 between MDA-MB-321 cancer cells and the normal MCF-10A cell line. Complexes 4-6 showed EC₅₀ values in the 1–10 μ M range in MDA-MB-231 cells, similar to cisplatin,⁴⁹ but above that range in DU-145 cells (Table 2). The data presented in Table 2 show that 2, 3, and 7 were essentially nontoxic in all of the three cell lines, with 3 showing the only EC₅₀ value below 25 μ M across the series in MDA-MB-231 cells. Complex 4, containing the thd ligand, was more toxic than 5 and 6 in MDA-MB-231, MCF-10A cell lines as well as in DU-145 cell lines (Table 2). Interestingly, complex 1 was the most toxic among all of the seven complexes toward all of the three cell lines but complex 7, having a similar structure with the addition of a carboxylic acid group (Figure 2), was nontoxic in all three cell lines (Table 2). Taken together, our results indicate that complex 1 was the most potent and effective in the series for obtaining selectivity for cancer cells. Although 4-6 were also active in the triple-negative breast and prostate cancer cells, they were just as or more potent in the normal breast epithelial line, which is common for many anticancer drugs.36

To understand the differential effects of 1-7 in cells, lipophilicities were determined (Table 2). Lipophilicity, measured as the partition coefficient between octanol and water $(\log P_{o/w})$, has been previously correlated with the cytotoxicity of Ru(II) complexes.⁵⁰ In these cases, higher $\log P_{o/w}$ values may indicate that compounds enter cells via passive diffusion, which may increase their cellular uptake and hence their toxicity. To test this hypothesis, a correlation between EC₅₀ of the complexes and their $\log P_{o/w}$ values was assessed and is shown in Figure 3. A scatter plot of $\log P_{o/w}$ vs EC₅₀ values for 1 and 3-6 resulted in a squared correlation coefficient (R^2) value of 0.8539, indicating that there was a moderate linear correlation between the efficacy and lipophilicity of 1 and 3-6 in MDA-MB-231 cells. Although complex 1 was the most potent and lipophilic in the series (Table 2), higher lipophilicity does not always lead to higher toxicity. We excluded compounds 2 and 7 from this analysis because their EC₅₀ values were >25 μ M (Table 2), and we were unable examine higher concentrations due to solubility limits of these compounds in the growth media. Therefore, it should be noted that compound 7, which is likely a neutral zwitterion at physiological pH, also possesses a high $\log P_{o/w}$ value but is not cytotoxic, indicating that not all compounds in the series that are lipophilic are cytotoxic. In contrast, no trend

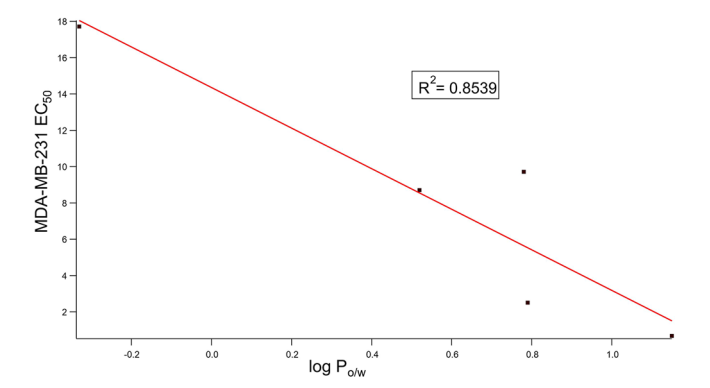


Figure 3. Scattered plot of EC₅₀ (μ M) in MDA-MB-231 cells of the complexes vs log $P_{\rm o/w}$.

was apparent between the EC_{50} values of the complexes and their redox potentials. For instance, complexes 1 and 4, which were the two most active compounds in MDA-MB-231 cells, showed $E_{1/2}$ values for Ru(III/II) couples of +0.73 and +0.60 V, respectively. Other complexes that were not active showed redox potentials between these two values.

To further understand the cellular behavior of our compounds, we examined the stability of 1–7 in cell growth media. Complexes were incubated in phenol red-free Dulbecco's modified Eagle's medium (DMEM) at 37 °C for 48 h, and their stability was assessed via electronic absorption spectroscopy (Figures S31–S37). These data showed no apparent shifts in absorption peaks that would indicate 1–7 undergo degradation events, such as thermal ligand exchange reactions or oxidation over the course of 48 h in cell growth media, that would influence their biological behavior.

Based on the data presented in Table 2, complexes 1 and 4 were identified as leads in EC_{50} determinations. To understand how 1 and 4 elicit their cytotoxicities, the mechanism of cell death was characterized. Cell death can occur through a variety of pathways, including apoptosis, necroptosis, and necrosis. Apoptosis is a form of programmed cell death that is known to be moderated by caspases. Morphological changes, which include cell shrinkage, condensation of the chromatin in the nucleus, and blebbing of the plasma membrane, are often associated with apoptosis. The cell membrane is generally not ruptured in apoptotic cells. Dysfunction of the mitochondria can lead to increased production of reactive

oxygen species (ROS) in cells, which include hydrogen peroxide, superoxide, and hydroxide radicals.⁵³ Increased ROS generally causes damage to biomolecules such as proteins, lipids, and nucleic acids, which eventually causes cell death by inducing apoptosis. 54 Necrosis, on the other hand, is a form of passive or uncontrolled cell death. Rupture of the cell membrane is a characteristic of necrosis, and the process is often induced by external agents or by deprivation of nutrients and oxygen.⁵⁵ Necroptosis is known as programmed necrosis and generally occurs in cells in which apoptosis is nonfunctional. Cell death by necroptosis is inhibited by necrostatin, an inhibitor of RIP-1 kinase, 56-59 Z-VAD-FMK is known to inhibit apoptotic cell death via caspase inactivation, 60-64 whereas N-acetylcysteine is a ROS quencher known to inhibit cell death due to the production of ROS. 65-69 An increase in viability of the cells when treated with any of these inhibitors in combination with a given drug in comparison to the drug alone provides evidence for the mechanism of cell death.7

To begin our studies, we evaluated the effects of necrostatin (10 μ M), Z-VAD-FMK (20 μ M), and N-acetylcysteine (5 mM) alone on MDA-MB-231 cells (Figure S29). Overall, these rescue agents were well tolerated by MDA-MB-231 cells, as judged by 72 h MTT analysis. When the cells were treated with 0.3 μ M of 1, the viability decreased to about 50% after 72 h. Cotreatment of the cells with 10 μ M necrostatin and 0.3 μ M 1 did not show a significant effect on cell viability, indicating that complex 1 does not induce necroptosis in MDA-MB-231 cells. However, statistically significant (P < 0.05) rescue from cell death was observed when the cells were treated with complex 1 (0.3 μ M) along with Z-VAD-FMK (20 μ M), consistent with 1 inducing apoptosis in MDA-MB-231 cells. A lower level of rescue was observed with N-acetylcysteine, implicating ROS in the mechanism of action for 1 (Figure 4). For complex 4 (2 μ M), no significant level of rescue from cell death was observed when the cells were co-treated with necrostatin (10 µM), Z-VAD-FMK (20 µM), or Nacetylcysteine (5 mM). Hence, the mechanism of cell death for complex 4 remains inconclusive from rescue experiments (Figure S30).

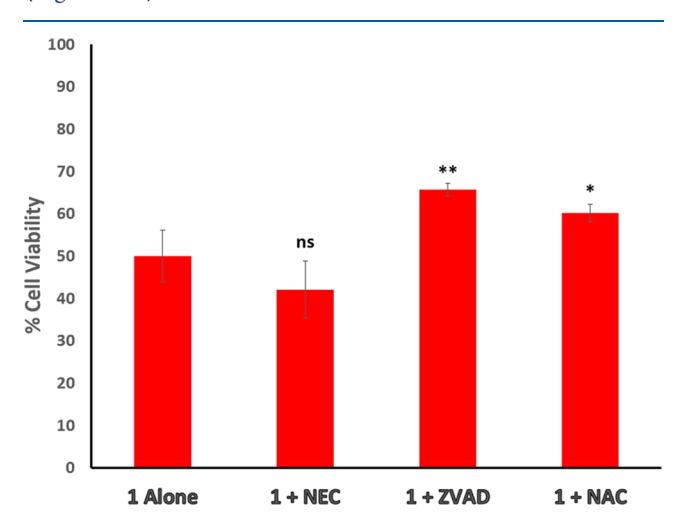


Figure 4. Viability of MDA-MB-231 cells treated with complex **1** (300 nM) alone or cotreated with necrostatin (10 μ M), Z-VAD-FMK (20 μ M), and *N*-acetylcysteine (5 mM) along with complex **1** (300 nM). *P* values are vs 300 nM complex **1**. ***P < 0.01, **P < 0.05, and *P < 0.10.

Mechanisms of cell death were investigated further with the aid of fluorescence-assisted cell sorting (FACS).74-76 In this study, MDA-MB-231 cells were treated with vehicle (1% DMSO), complex 1 (300 nM or 1 μ M; Figure 5B,C), complex 4 (3 or 6 μ M; Figure 5E,F), or H₂O₂ (500 mM), which served as a positive control for necrosis. ^{77,78} MDA-MB-231 cells were stained with annexin V and propidium iodide. Annexin V is known to bind with phosphatidylserine on the outer leaflet of the cell plasma membrane, which is associated with apoptosis.⁷⁹ Propidium iodide is a dye that is generally nonpermeable to cells but can enter the cell if the plasma membrane is compromised. 80 Early stages of apoptosis do not involve the destruction of the plasma membrane and therefore propidium iodide uptake is not seen in early apoptotic cells. However, necrosis is known to cause permeabilization of the cell membrane, such that necrotic cells are known for uptake of both Annexin V and propidium iodide (PI). FACS studies show a concentration-dependent shift in cell population to the lower right quadrant (Annexin V positive, PI negative) for cells treated with complexes 1 and 4 compared to the vehicle. Although higher concentrations of 1 and 4 were required to observe apoptosis via FACS as compared to the 96-well experiments, a significant shift of the cell population to the lower right quadrant was observed for complexes 1 and 4. Taken together, these results establish evidence that both complexes 1 and 4 induced apoptosis in MDA-MB-231 cells.

DISCUSSION

In this paper, we describe the biological evaluation of seven Ru(II) polypyridyl complexes containing acac ligands against two cancerous cell lines, MDA-MB-231 and DU-145 and one noncancerous cell line, MCF-10A. Our data reveal that one of our complexes (complex 1) showed nanomolar potency and was 2.5 times more selective toward MDA-MB-231 cell lines as compared to MCF-10A cell lines. Previous data on Ru naphthoquinone complexes incorporated with phosphorousbased ligands have shown excellent selectivity toward MDA-MB-231 cells as compared to MCF-10A cells.⁸¹ Selectivity toward MDA-MB-231 over MCF-10A cells was also seen by several reported Ru phosphine/mercapto complexes, though to a much lesser extent. 82 However, studies on other Ru polypyridyl complexes with acac-based ferrocenyl β -diketonate ligands showed no selectivity toward cancerous HCT116 p53^{+/+} cells over noncancerous ARPE-19 cells.³⁶ Similarly, other studies on bpy-based Ru complexes with similar acacbased ligands showed higher toxicity compared to our complexes when tested against cancerous cell lines like HL60, MIA PaCa-2, and DU-145 cells, but no studies regarding selectivity of these complexes toward cancerous vs non-cancerous cell lines have been mentioned by the authors.³⁹ Reports on cancer cell selectivity have also not been reported with Ru(II) polypyridyl complexes containing acac-based ligand curcumin and Ru(II) polypyridyl complexes containing D-glucose and D-fructose conjugated acac-based ligands. ^{37,38} Therefore, we can say that complex 1 is currently the only known acac-based Ru polypyridyl complex, which shows selectivity for a cancerous vs normal cell line.

CONCLUSIONS

In conclusion, seven Ru(II) polypyridyl complexes containing acac and substituted acac ligands were synthesized and characterized. Two complexes, 1 and 4, showed promising

Inorganic Chemistry Article pubs.acs.org/IC

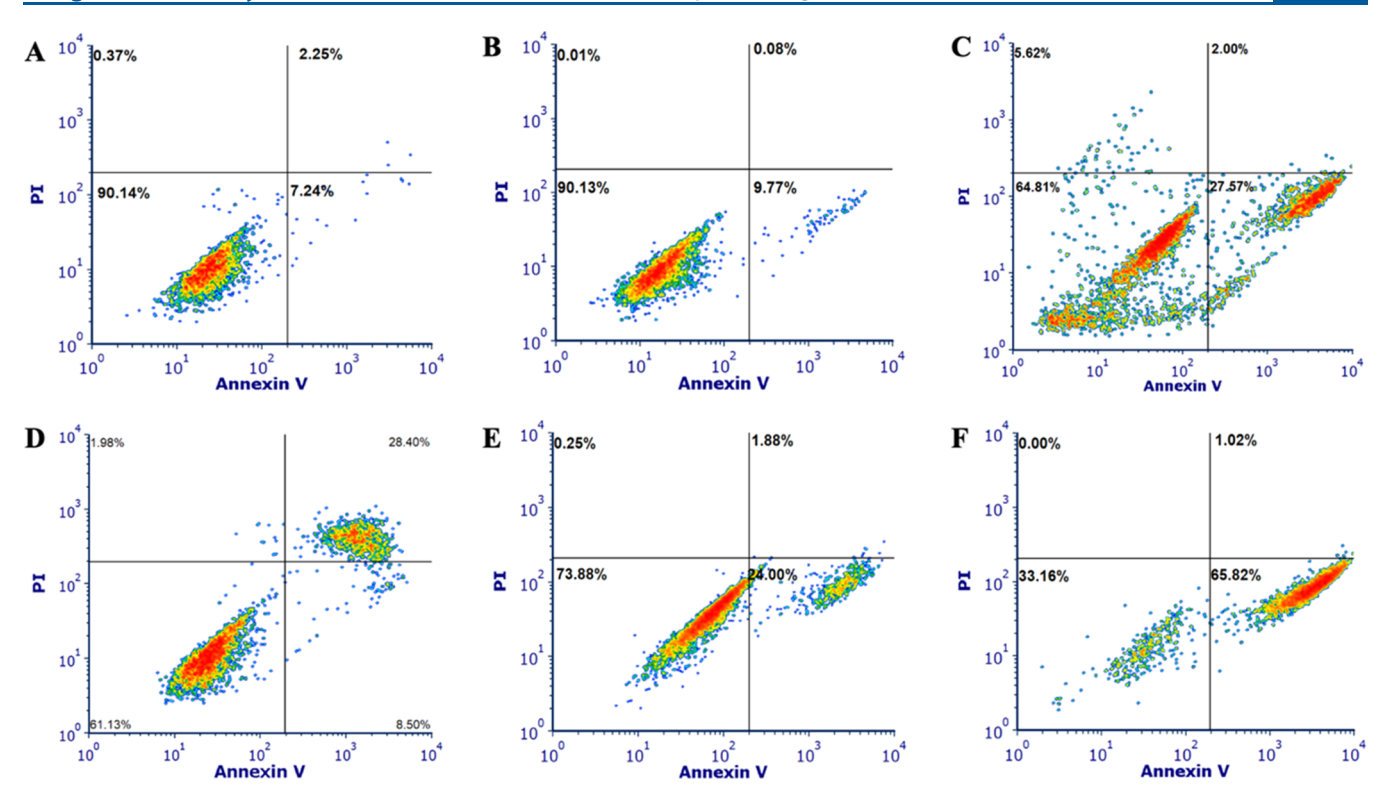


Figure 5. Flow cytometric analysis of MDA-MB-231 cells after 72 h treatment with 1 or 4 using annexin V/propidium iodide staining. Treatment conditions: (A) vehicle; (B) 1 (300 nM); (C) 1 (1 μM); (D) H₂O₂ (500 mM), 3 h treatment; (E) 4 (3 μM); and (F) 4 (6 μM). Data are indicative of three independent experiments.

activity in breast and prostate cancer cell lines. Complex 1 was more toxic toward DU-145 and MDA-MB-231 cell lines compared to MCF-10A cells. Complex 4, on the other hand, was toxic toward MDA-MB-231 and MCF-10A cell lines but not toward DU-145 cell lines. Importantly, complex 1 was also found to be up to 2.5 times more selective toward MDA-MB-231 triple-negative breast cancer cells than MCF-10A normal breast epithelial cells. This level of selectivity is important since, for example, cisplatin does not exhibit any selectivity between MDA-MB-231 and MCF-10A cells. 83,84 Studies on the mechanism of cell death for complexes 1 and 4 established that both complexes induced apoptosis in MDA-MB-231 cells, as judged by rescue experiments and FACS analysis. These results are encouraging and warrant further modification of 1 to increase its selectivity toward cancer cells.

ASSOCIATED CONTENT

Solution Supporting Information

The Supporting Information is available free of charge at https://pubs.acs.org/doi/10.1021/acs.inorgchem.1c02796.

¹H NMR spectra and ESI mass spectra for complexes 1-7, cyclic voltammograms for complexes 1-7, biological characterization data, and stability of complexes 1-7 (PDF)

■ AUTHOR INFORMATION

Corresponding Authors

Claudia Turro - Department of Chemistry and Biochemistry, The Ohio State University, Columbus, Ohio 43210, United States; orcid.org/0000-0003-3202-5870; Email: turro.1@osu.edu

Jeremy J. Kodanko – Department of Chemistry, Wayne State University, Detroit, Michigan 48202, United States; orcid.org/0000-0001-5196-7463; Email: jkodanko@ chem.wayne.edu

Authors

Sayak Gupta - Department of Chemistry, Wayne State University, Detroit, Michigan 48202, United States Jessica M. Vandevord - Department of Chemistry and Biochemistry, The Ohio State University, Columbus, Ohio 43210, United States

Lauren M. Loftus - Department of Chemistry and Biochemistry, The Ohio State University, Columbus, Ohio 43210, United States

Nicholas Toupin - Department of Chemistry, Wayne State University, Detroit, Michigan 48202, United States

Malik H. Al-Afyouni - Department of Chemistry and Biochemistry, The Ohio State University, Columbus, Ohio 43210, United States

Thomas N. Rohrabaugh, Jr. - Department of Chemistry and Biochemistry, The Ohio State University, Columbus, Ohio 43210, United States

Complete contact information is available at: https://pubs.acs.org/10.1021/acs.inorgchem.1c02796

Notes

The authors declare no competing financial interest.

ACKNOWLEDGMENTS

The authors gratefully acknowledge the National Science Foundation (CHE 2102508) and Wayne State University for support of this research. For instrumentation support, the

authors thank the Hütteman laboratory and Penrose Therapeu T_v .

REFERENCES

- (1) Bray, F.; Ferlay, J.; Soerjomataram, I.; Siegel, R. L.; Torre, L. A.; Jemal, A. Global cancer statistics 2018: GLOBOCAN estimates of incidence and mortality worldwide for 36 cancers in 185 countries. *CA: Cancer J. Clin.* **2018**, *68*, 394–424.
- (2) Schirrmacher, V. From chemotherapy to biological therapy: A review of novel concepts to reduce the side effects of systemic cancer treatment. *Int. J. Oncol.* **2019**, *54*, 407–419.
- (3) Oun, R.; Moussa, Y. E.; Wheate, N. J. The side effects of platinum-based chemotherapy drugs: a review for chemists. *Dalton Trans.* **2018**, 47, 6645–6653.
- (4) Johnstone, T. C.; Suntharalingam, K.; Lippard, S. J. The next generation of platinum drugs: targeted Pt (II) agents, nanoparticle delivery, and Pt (IV) prodrugs. *Chem. Rev.* **2016**, *116*, 3436–3486.
- (5) Aris, S. M.; Farrell, N. P. Towards antitumor active transplatinum compounds. Eur. J. Inorg. Chem. 2009, 2009, 1293.
- (6) van Rijt, S. H.; Sadler, P. J. Current applications and future potential for bioinorganic chemistry in the development of anticancer drugs. *Drug Discovery Today* **2009**, *14*, 1089–1097.
- (7) Allardyce, C. S.; Dyson, P. J. Metal-based drugs that break the rules. *Dalton Trans.* **2016**, *45*, 3201–3209.
- (8) Barry, N. P.; Sadler, P. J. Exploration of the medical periodic table: towards new targets. *Chem. Commun.* **2013**, *49*, 5106–5131.
- (9) Peña, B.; David, A.; Pavani, C.; Baptista, M. S.; Pellois, J.-P.; Turro, C.; Dunbar, K. R. Cytotoxicity studies of cyclometallated ruthenium (II) compounds: New applications for ruthenium dyes. *Organometallics* **2014**, *33*, 1100–1103.
- (10) Coverdale, J. P.; Laroiya-McCarron, T.; Romero-Canelón, I. Designing ruthenium anticancer drugs: What have we learnt from the key drug candidates? *Inorganics* **2019**, *7*, No. 31.
- (11) Gasser, G.; Ott, I.; Metzler-Nolte, N. Organometallic anticancer compounds. *J. Med. Chem.* **2011**, *54*, 3–25.
- (12) Mari, C.; Pierroz, V.; Ferrari, S.; Gasser, G. Combination of Ru (II) complexes and light: new frontiers in cancer therapy. *Chem. Sci.* **2015**, *6*, 2660–2686.
- (13) Boros, E.; Dyson, P. J.; Gasser, G. Classification of metal-based drugs according to their mechanisms of action. *Chem* **2020**, *6*, 41–60.
- (14) Clarke, M. J. Ruthenium metallopharmaceuticals. *Coord. Chem. Rev.* 2002, 232, 69–93.
- (15) Yan, Y. K.; Melchart, M.; Habtemariam, A.; Sadler, P. J. Organometallic chemistry, biology and medicine: ruthenium arene anticancer complexes. *Chem. Commun.* **2005**, 4764–4776.
- (16) Bruijnincx, P. C.; Sadler, P. J. New trends for metal complexes with anticancer activity. *Curr. Opin. Chem. Biol.* **2008**, *12*, 197–206.
- (17) Knoll, J. D.; Turro, C. Control and utilization of ruthenium and rhodium metal complex excited states for photoactivated cancer therapy. *Coord. Chem. Rev.* **2015**, 282–283, 110–126.
- (18) Zeng, L.; Gupta, P.; Chen, Y.; Wang, E.; Ji, L.; Chao, H.; Chen, Z.-S. The development of anticancer ruthenium (II) complexes: from single molecule compounds to nanomaterials. *Chem. Soc. Rev.* **2017**, 46, 5771–5804.
- (19) Bergamo, A.; Sava, G. Ruthenium anticancer compounds: myths and realities of the emerging metal-based drugs. *Dalton Trans.* **2011**, 40, 7817–7823.
- (20) Bijelic, A.; Theiner, S.; Keppler, B. K.; Rompel, A. X-ray structure analysis of indazolium trans-[tetrachlorobis (1 H-indazole) ruthenate (III)](KP1019) bound to human serum albumin reveals two ruthenium binding sites and provides insights into the drug binding mechanism. *J. Med. Chem.* **2016**, *59*, 5894–5903.
- (21) Brabec, V.; Nováková, O. DNA binding mode of ruthenium complexes and relationship to tumor cell toxicity. *Drug Resist. Updates* **2006**, *9*, 111–122.
- (22) Gill, M. R.; Thomas, J. A. Ruthenium (II) polypyridyl complexes and DNA—from structural probes to cellular imaging and therapeutics. *Chem. Soc. Rev.* **2012**, *41*, 3179–3192.

- (23) Kapitza, S.; Pongratz, M.; Jakupec, M.; Heffeter, P.; Berger, W.; Lackinger, L.; Keppler, B.; Marian, B. Heterocyclic complexes of ruthenium (III) induce apoptosis in colorectal carcinoma cells. *J. Cancer Res. Clin. Oncol.* **2005**, *131*, 101–110.
- (24) Sava, G.; Frausin, F.; Cocchietto, M.; Vita, F.; Podda, E.; Spessotto, P.; Furlani, A.; Scarcia, V.; Zabucchi, G. Actin-dependent tumour cell adhesion after short-term exposure to the antimetastasis ruthenium complex NAMI-A. *Eur. J. Cancer* **2004**, *40*, 1383–1396.
- (25) Monro, S.; Colón, K. L.; Yin, H.; Roque, J., III; Konda, P.; Gujar, S.; Thummel, R. P.; Lilge, L.; Cameron, C. G.; McFarland, S. A. Transition metal complexes and photodynamic therapy from a tumor-centered approach: challenges, opportunities, and highlights from the development of TLD1433. *Chem. Rev.* 2019, 119, 797–828.
- (26) Chamberlain, S.; Cole, H. D.; Roque, J.; Bellnier, D.; McFarland, S. A.; Shafirstein, G. TLD1433-Mediated photodynamic therapy with an optical surface applicator in the treatment of lung cancer cells in vitro. *Pharmaceuticals* **2020**, *13*, No. 137.
- (27) Rausch, M.; Dyson, P. J.; Nowak-Sliwinska, P. Recent Considerations in the Application of RAPTA-C for Cancer Treatment and Perspectives for Its Combination with Immunotherapies. *Adv. Ther.* **2019**, *2*, No. 1900042.
- (28) Dwyer, F.; Mayhew, E.; Roe, E.; Shulman, A. Inhibition of landschuetz ascites tumour growth by metal chelates derived from 3, 4, 7, 8-tetramethyl-1, 10-phenanthroline. *Br. J. Cancer* **1965**, *19*, 195.
- (29) Hu, P.; Wang, Y.; Zhang, Y.; Song, H.; Gao, F.; Lin, H.; Wang, Z.; Wei, L.; Yang, F. Novel mononuclear ruthenium (II) complexes as potent and low-toxicity antitumour agents: synthesis, characterization, biological evaluation and mechanism of action. *RSC Adv.* **2016**, *6*, 29963–29976.
- (30) Munteanu, A. C.; Notaro, A.; Jakubaszek, M.; Cowell, J.; Tharaud, M.; Goud, B.; Uivarosi, V.; Gasser, G. Synthesis, Characterization, Cytotoxic Activity, and Metabolic Studies of Ruthenium(II) Polypyridyl Complexes Containing Flavonoid Ligands. *Inorg. Chem.* **2020**, *59*, 4424–4434.
- (31) Notaro, A.; Jakubaszek, M.; Koch, S.; Rubbiani, R.; Domotor, O.; Enyedy, E. A.; Dotou, M.; Bedioui, F.; Tharaud, M.; Goud, B.; Ferrari, S.; Alessio, E.; Gasser, G. A Maltol-Containing Ruthenium Polypyridyl Complex as a Potential Anticancer Agent. *Chem. Eur. J.* **2020**, *26*, 4997–5009.
- (32) Notaro, A.; Jakubaszek, M.; Rotthowe, N.; Maschietto, F.; Vinck, R.; Felder, P. S.; Goud, B.; Tharaud, M.; Ciofini, I.; Bedioui, F.; Winter, R. F.; Gasser, G. Increasing the Cytotoxicity of Ru(II) Polypyridyl Complexes by Tuning the Electronic Structure of Dioxo Ligands. J. Am. Chem. Soc. 2020, 142, 6066–6084.
- (33) Oliveira, R. M.; de Souza Daniel, J. F.; Carlos, R. M. Synthesis, spectroscopic characterization and biological activity of cis-[Ru (hesperidin)(1, 10'-phenanthroline) 2](PF6) complex. *J. Mol. Struct.* **2013**, *1031*, 269–274.
- (34) Shulman, A.; Laycock, G. M.; Bradley, T. Action of 1, 10-phenanthroline transition metal chelates on P388 mouse lymphocytic leukaemic cells. *Chem.-Biol. Interact.* 1977, *16*, 89–99.
- (35) Zahirović, A.; Kahrović, E.; Cindrić, M.; Kraljević Pavelić, S.; Hukić, M.; Harej, A.; Turkušić, E. Heteroleptic ruthenium bioflavonoid complexes: from synthesis to in vitro biological activity. *J. Coord. Chem.* **2017**, *70*, 4030–4053.
- (36) Allison, M.; Caramés-Méndez, P.; Pask, C. M.; Phillips, R. M.; Lord, R. M.; McGowan, P. C. Bis (bipyridine) ruthenium (II) ferrocenyl β -diketonate complexes: exhibiting nanomolar potency against human cancer cell lines. *Chem. Eur. J.* **2021**, *27*, 3737–3744.
- (37) Li, S.; Xu, G.; Zhu, Y.; Zhao, J.; Gou, S. Bifunctional ruthenium(ii) polypyridyl complexes of curcumin as potential anticancer agents. *Dalton Trans.* **2020**, *49*, 9454–9463.
- (38) Pröhl, M.; Bus, T.; Czaplewska, J. A.; Traeger, A.; Deicke, M.; Weiss, H.; Weigand, W.; Schubert, U. S.; Gottschaldt, M. Synthesis and in vitro Toxicity ofd-Glucose andd-Fructose Conjugated Curcumin-Ruthenium Complexes. *Eur. J. Inorg. Chem.* **2016**, 2016, 5197–5204.
- (39) Ryan, R. T.; Havrylyuk, D.; Stevens, K. C.; Moore, L. H.; Parkin, S.; Blackburn, J. S.; Heidary, D. K.; Selegue, J. P.; Glazer, E. C.

- Biological Investigations of Ru(II) Complexes With Diverse betadiketone Ligands. Eur. J. Inorg. Chem. 2021, 2021, 3611-3621.
- (40) Loftus, L. M.; Al-Afyouni, K. F.; Turro, C. New RuII Scaffold for Photoinduced Ligand Release with Red Light in the Photodynamic Therapy (PDT) Window. *Chem. Eur. J.* **2018**, *24*, 11550–11553
- (41) Al-Afyouni, M. H.; Rohrabaugh, T. N.; Al-Afyouni, K. F.; Turro, C. New Ru (II) photocages operative with near-IR light: new platform for drug delivery in the PDT window. *Chem. Sci.* **2018**, *9*, 6711–6720.
- (42) Lee, Y. Y.; Walker, D. B.; Gooding, J. J.; Messerle, B. A. Ruthenium (ii) complexes containing functionalised β -diketonate ligands: developing a ferrocene mimic for biosensing applications. *Dalton Trans.* **2014**, 43, 12734–12742.
- (43) Li, M.; Sheth, S.; Xu, Y.; Song, Q. Ru (II)-bipyridine complex as a highly sensitive luminescent probe for Cu2+ detection and cell imaging. *Microchem. J.* **2020**, *156*, No. 104848.
- (44) Fulmer, G. R.; Miller, A. J. M.; Sherden, N. H.; Gottlieb, H. E.; Nudelman, A.; Stoltz, B. M.; Bercaw, J. E.; Goldberg, K. I. NMR Chemical Shifts of Trace Impurities: Common Laboratory Solvents, Organics, and Gases in Deuterated Solvents Relevant to the Organometallic Chemist. *Organometallics* **2010**, *29*, 2176–2179.
- (45) l-Hendawy, A. M.; Al-Kubaisi, A. H.; Al-Madfa, H. A. Ruthenium (II) and (III) bipyridine complexes and their catalytic oxidation properties for organic compounds. *Polyhedron* **1997**, *16*, 3039–3045.
- (46) Fetzer, L.; Boff, B.; Ali, M.; Xiangjun, M.; Collin, J.-P.; Sirlin, C.; Gaiddon, C.; Pfeffer, M. Library of second-generation cycloruthenated compounds and evaluation of their biological properties as potential anticancer drugs: Passing the nanomolar barrier. *Dalton Trans.* **2011**, *40*, 8869–8878.
- (47) Juris, A.; Balzani, V.; Barigelletti, F.; Campagna, S.; Belser, Pl.; von Zelewsky, Av. Ru (II) polypyridine complexes: photophysics, photochemistry, eletrochemistry, and chemiluminescence. *Coord. Chem. Rev.* **1988**, *84*, 85–277.
- (48) Rachford, A. A.; Petersen, J. L.; Rack, J. J. Designing molecular bistability in ruthenium dimethyl sulfoxide complexes. *Inorg. Chem.* **2005**, *44*, 8065–8075.
- (49) Mazur, M.; Mrozowicz, M.; Buchowicz, W.; Koszytkowska-Stawińska, M.; Kamiński, R.; Ochal, Z.; Wińska, P.; Bretner, M. Formylation of a metathesis-derived ansa [4]-ferrocene: a simple route to anticancer organometallics. *Dalton Trans.* **2020**, *49*, 11504–11511.
- (50) Poynton, F. E.; Bright, S. A.; Blasco, S.; Williams, D. C.; Kelly, J. M.; Gunnlaugsson, T. The development of ruthenium (II) polypyridyl complexes and conjugates for in vitro cellular and in vivo applications. *Chem. Soc. Rev.* **2017**, *46*, 7706–7756.
- (51) Thornberry, N. A. Caspases: key mediators of apoptosis. *Chem. Biol.* **1998**, *5*, R97–R103.
- (52) Elmore, S. Apoptosis: a review of programmed cell death. *Toxicol. Pathol.* **2007**, *35*, 495–516.
- (53) Georgieva, E.; Ivanova, D.; Zhelev, Z.; Bakalova, R.; Gulubova, M.; Aoki, I. Mitochondrial dysfunction and redox imbalance as a diagnostic marker of "free radical diseases". *Anticancer Res.* **2017**, *37*, 5373–5381
- (54) Redza-Dutordoir, M.; Averill-Bates, D. A. Activation of apoptosis signalling pathways by reactive oxygen species. *Biochim. Biophys. Acta, Mol. Cell Res.* **2016**, *1863*, 2977–2992.
- (55) Nirmala, J. G.; Lopus, M. Cell death mechanisms in eukaryotes. *Cell Biol. Toxicol.* **2020**, *36*, 145–164.
- (56) Dhuriya, Y. K.; Sharma, D. Necroptosis: a regulated inflammatory mode of cell death. *J. Neuroinflammation* **2018**, *15*, No. 199.
- (57) Zheng, W.; Degterev, A.; Hsu, E.; Yuan, J.; Yuan, C. Structure—activity relationship study of a novel necroptosis inhibitor, necrostatin-7. *Bioorg. Med. Chem. Lett.* **2008**, *18*, 4932–4935.
- (58) Smith, C. C.; Yellon, D. M. Necroptosis, necrostatins and tissue injury. J. Cell. Mol. Med. 2011, 15, 1797–1806.

- (59) Han, W.; Xie, J.; Li, L.; Liu, Z.; Hu, X. Necrostatin-1 reverts shikonin-induced necroptosis to apoptosis. *Apoptosis* **2009**, *14*, 674–686
- (60) Fransolet, M.; Noël, L.; Henry, L.; Labied, S.; Blacher, S.; Nisolle, M.; Munaut, C. Evaluation of Z-VAD-FMK as an antiapoptotic drug to prevent granulosa cell apoptosis and follicular death after human ovarian tissue transplantation. *J. Assist. Reprod. Genet.* **2019**, *36*, 349–359.
- (61) Egger, L.; Schneider, J.; Rheme, C.; Tapernoux, M.; Häcki, J.; Borner, C. Serine proteases mediate apoptosis-like cell death and phagocytosis under caspase-inhibiting conditions. *Cell Death Differ.* **2003**, *10*, 1188–1203.
- (62) Henry, L.; Fransolet, M.; Labied, S.; Blacher, S.; Masereel, M.-C.; Foidart, J.-M.; Noel, A.; Nisolle, M.; Munaut, C. Supplementation of transport and freezing media with anti-apoptotic drugs improves ovarian cortex survival. *J. Ovarian Res.* **2016**, *9*, No. 4.
- (63) Zhang, X.; Liu, S.; Guo, C.; Zong, J.; Sun, M.-Z. The association of annexin A2 and cancers. Clin. Transl. Oncol. 2012, 14, 634–640
- (64) Li, M.; Kondo, T.; Zhao, Q.-L.; Li, F.-J.; Tanabe, K.; Arai, Y.; Zhou, Z.-C.; Kasuya, M. Apoptosis induced by cadmium in human lymphoma U937 cells through Ca2+-calpain and caspase-mitochondria-dependent pathways. *J. Biol. Chem.* **2000**, 275, 39702–39709.
- (65) Malik, F.; Kumar, A.; Bhushan, S.; Khan, S.; Bhatia, A.; Suri, K. A.; Qazi, G. N.; Singh, J. Reactive oxygen species generation and mitochondrial dysfunction in the apoptotic cell death of human myeloid leukemia HL-60 cells by a dietary compound withaferin A with concomitant protection by N-acetyl cysteine. *Apoptosis* **2007**, *12*, 2115–2133.
- (66) Oh, S.-H.; Lim, S.-C. A rapid and transient ROS generation by cadmium triggers apoptosis via caspase-dependent pathway in HepG2 cells and this is inhibited through N-acetylcysteine-mediated catalase upregulation. *Toxicol. Appl. Pharmacol.* **2006**, *212*, 212–223.
- (67) Chen, S.; Ren, Q.; Zhang, J.; Ye, Y.; Zhang, Z.; Xu, Y.; Guo, M.; Ji, H.; Xu, C.; Gu, C.; et al. N-acetyl-L-cysteine protects against cadmium-induced neuronal apoptosis by inhibiting ROS-dependent activation of A kt/m TOR pathway in mouse brain. *Neuropathol. Appl. Neurobiol.* 2014, 40, 759–777.
- (68) Wang, J.-P.; Hsieh, C.-H.; Liu, C.-Y.; Lin, K.-H.; Wu, P.-T.; Chen, K.-M.; Fang, K. Reactive oxygen species-driven mitochondrial injury induces apoptosis by teroxirone in human non-small cell lung cancer cells. *Oncol. Lett.* **2017**, *14*, 3503–3509.
- (69) Venkataramana, M.; Nayaka, S. C.; Anand, T.; Rajesh, R.; Aiyaz, M.; Divakara, S.; Murali, H.; Prakash, H.; Rao, P. L. Zearalenone induced toxicity in SHSY-5Y cells: the role of oxidative stress evidenced by N-acetyl cysteine. *Food Chem. Toxicol.* **2014**, *65*, 335–342.
- (70) Hong, Y.; Fan, D. Ginsenoside Rk1 induces cell cycle arrest and apoptosis in MDA-MB-231 triple negative breast cancer cells. *Toxicology* **2019**, *418*, 22–31.
- (71) Park, E.; Min, K.; Lee, T.; Yoo, Y.; Kim, Y.; Kwon, T. β -Lapachone induces programmed necrosis through the RIP1-PARP-AIF-dependent pathway in human hepatocellular carcinoma SK-Hep1 cells. *Cell Death Dis.* **2014**, *5*, No. e1230.
- (72) Sunilkumar, D.; Drishya, G.; Chandrasekharan, A.; Shaji, S. K.; Bose, C.; Jossart, J.; Perry, J. J. P.; Mishra, N.; Kumar, G. B.; Nair, B. G. Oxyresveratrol drives caspase-independent apoptosis-like cell death in MDA-MB-231 breast cancer cells through the induction of ROS. *Biochem. Pharmacol.* **2020**, *173*, No. 113724.
- (73) Banerjee, M.; Chattopadhyay, S.; Choudhuri, T.; Bera, R.; Kumar, S.; Chakraborty, B.; Mukherjee, S. K. Cytotoxicity and cell cycle arrest induced by andrographolide lead to programmed cell death of MDA-MB-231 breast cancer cell line. *J. Biomed. Sci.* **2016**, 23, No. 40.
- (74) Toupin, N. P.; Nadella, S.; Steinke, S. J.; Turro, C.; Kodanko, J. J. Dual-Action Ru (II) Complexes with Bulky π -Expansive Ligands: Phototoxicity without DNA Intercalation. *Inorg. Chem.* **2020**, *59*, 3919–3933.

- (75) Balaji, S.; Mohamed Subarkhan, M. K.; Ramesh, R.; Wang, H.; Semeril, D. Synthesis and structure of arene Ru (II) N∧ O-chelating complexes: in vitro cytotoxicity and cancer cell death mechanism. *Organometallics* **2020**, *39*, 1366–1375.
- (76) Osawa, T.; Davies, D.; Hartley, J. Mechanism of cell death resulting from DNA interstrand cross-linking in mammalian cells. *Cell Death Dis.* **2011**, *2*, No. e187.
- (77) Zhao, L.; Lin, H.; Chen, S.; Chen, S.; Cui, M.; Shi, D.; Wang, B.; Ma, K.; Shao, Z. Hydrogen peroxide induces programmed necrosis in rat nucleus pulposus cells through the RIP1/RIP3-PARP-AIF pathway. *J. Orthop. Res.* **2018**, *36*, 1269–1282.
- (78) Matteucci, C.; Grelli, S.; De Smaele, E.; Fontana, C.; Mastino, A. Identification of nuclei from apoptotic, necrotic, and viable lymphoid cells by using multiparameter flow cytometry. *Cytom.: J. Int. Soc. Anal. Cytol.* **1999**, *35*, 145–153.
- (79) Zhang, J.-M.; Li, L.-X.; Yang, Y.-X.; Liu, X.-L.; Wan, X.-P. Is caspase inhibition a valid therapeutic strategy in cryopreservation of ovarian tissue? *J. Assist. Reprod. Genet.* **2009**, *26*, 415–420.
- (80) Ling, E.; Shirai, K.; Kanekatsu, R.; Kiguchi, K. Classification of larval circulating hemocytes of the silkworm, Bombyx mori, by acridine orange and propidium iodide staining. *Histochem. Cell Biol.* **2003**, *120*, 505–511.
- (81) Oliveira, K. M.; Peterson, E. J.; Carroccia, M. C.; Cominetti, M. R.; Deflon, V. M.; Farrell, N. P.; Batista, A. A.; Correa, R. S. Ru(II)-Naphthoquinone complexes with high selectivity for triple-negative breast cancer. *Dalton Trans.* **2020**, *49*, 16193–16203.
- (82) Ribeiro, G. H.; Guedes, A. P. M.; de Oliveira, T. D.; de Correia, C.; Colina-Vegas, L.; Lima, M. A.; Nobrega, J. A.; Cominetti, M. R.; Rocha, F. V.; Ferreira, A. G.; Castellano, E. E.; Teixeira, F. R.; Batista, A. A. Ruthenium(II) Phosphine/Mercapto Complexes: Their in Vitro Cytotoxicity Evaluation and Actions as Inhibitors of Topoisomerase and Proteasome Acting as Possible Triggers of Cell Death Induction. *Inorg. Chem.* **2020**, *59*, 15004–15018.
- (83) Vaidergorn, M. M.; Carneiro, Z. A.; Lopes, C. D.; de Albuquerque, S.; Reis, F. C.; Nikolaou, S.; e Mello, J. F.; Genesi, G. L.; Trossini, G. H.; Ganesan, A.; et al. β -amino alcohols and their respective 2-phenyl-N-alkyl aziridines as potential DNA minor groove binders. *Eur. J. Med. Chem.* **2018**, *157*, 657–664.
- (84) de Oliveira, L. P.; Carneiro, Z. A.; Ribeiro, C. M.; Lima, M. F.; Paixão, D. A.; Pivatto, M.; de Souza, M. V.; Teixeira, L. R.; Lopes, C. D.; de Albuquerque, S.; et al. Three new platinum complexes containing fluoroquinolones and DMSO: Cytotoxicity and evaluation against drug-resistant tuberculosis. *J. Inorg. Biochem.* **2018**, *183*, 77–83.